

This is an Open Access document downloaded from ORCA, Cardiff University's institutional repository:<https://orca.cardiff.ac.uk/id/eprint/134791/>

This is the author's version of a work that was submitted to / accepted for publication.

Citation for final published version:

Al-Jumaa, Maha, Hallett, Maurice B and Dewitt, Sharon 2020. Cell surface topography controls phagocytosis and cell spreading: the membrane reservoir in neutrophils. *Biochimica et Biophysica Acta (BBA) - Molecular Cell Research* 12 , 118832. 10.1016/j.bbamcr.2020.118832

Publishers page: <http://dx.doi.org/10.1016/j.bbamcr.2020.118832>

Please note:

Changes made as a result of publishing processes such as copy-editing, formatting and page numbers may not be reflected in this version. For the definitive version of this publication, please refer to the published source. You are advised to consult the publisher's version if you wish to cite this paper.

This version is being made available in accordance with publisher policies. See <http://orca.cf.ac.uk/policies.html> for usage policies. Copyright and moral rights for publications made available in ORCA are retained by the copyright holders.



## **Cell surface topography controls phagocytosis and cell spreading: the membrane reservoir in neutrophils**

Maha Al-Jumaa<sup>1)</sup>, Maurice B. Hallett<sup>1</sup> and Sharon Dewitt<sup>2</sup>

<sup>1</sup>Neutrophil Signalling Group, Cardiff University School of Medicine, Cardiff CF14 4XN, UK

<sup>2</sup> Matrix Biology & Tissue Repair Research Unit, College of Biomedical and Life Sciences, School of Dentistry, Cardiff University, Cardiff CF14 4XY, UK

Running title: Membrane tension and phagocytosis

Corresponding author: S Dewitt, Cardiff University School of Dentistry, Cardiff CF14 4XY, UK

Email: Dewitt@cardiff.ac.uk

Tel: +44 (0)29 2251 0665

**Summary statement:** The surface topography of neutrophils was shown to provide the membrane reservoir for apparent cell surface expansion during phagocytosis and cell spreading, as shown by analysis of the mechanism by which osmotic hyperwrinkling of the cell surface prevents these cellular events.

---

<sup>1)</sup> Present address: King Abdullah International Medical Research Centre, Riyadh, Saudi Arabia.

## **Abstract**

Neutrophils exhibit rapid cell spreading and phagocytosis, both requiring a large apparent increase in the cell surface area. The wrinkled surface topography of these cells may provide the membrane reservoir for this. Here, the effects of manipulation of the neutrophil cell surface topography on phagocytosis and cell spreading were established. Chemical expansion of the plasma membrane or osmotic swelling had no effects. However, osmotic shrinking of neutrophils inhibited both cell spreading and phagocytosis. Triggering a  $\text{Ca}^{2+}$  signal in osmotically shrunk cells (by  $\text{IP}_3$  uncaging) evoked tubular blebs instead of full cell spreading. Phagocytosis was halted at the phagocytic cup stage by osmotic shrinking induced after the phagocytic  $\text{Ca}^{2+}$  signalling. Restoration of isotonicity was able to restore complete phagocytosis. These data thus provide evidence that the wrinkled neutrophil surface topography provides the membrane reservoir to increase the available cell surface area for phagocytosis and spreading by neutrophils. (146 words)

**Keywords:** phagocytosis: cell spreading: cell surface topography: neutrophil: cytosolic  $\text{Ca}^{2+}$

## **Introduction**

Phagocytosis and cell spreading are related cellular phenomena. Indeed, the spreading of neutrophils on a planar surface is often considered as “frustrated phagocytosis”. In both cases, there is an apparent massive increase in cell surface area, calculated to be about 200-300% of the initial cell surface area [1, 2, 3, 4]. However, during this process, there is no increase in the total amount of plasma membrane as monitored by FM1-43 inclusion into the membrane [5] which suggests that wrinkles in the cell surface may unfold to provide the additional membrane. A similar conclusion has been reached for macrophage phagocytosis by measurement of whole cell capacitance [6] or FM 1-43 [7]. Micropipette aspiration techniques to measure cell surface tension have shown that the wrinkled neutrophil membrane is held in place by a “molecular velcro” [8] with about 25% of the wrinkled surface being held loosely (slack component), and the majority of wrinkles being held firmly [8, 9]. The firm maintenance of the wrinkles is the result of proteins which cross link the plasma membrane to the underlying actin cortex, notably ezrin [10, 11, 12]. The strength of these wrinkles is reduced during phagocytosis [8] when an elevation of cytosolic  $Ca^{2+}$  occurs [13]. Phagocytosis and cell spreading are both dependent on the activation of the  $Ca^{2+}$ -activated protease calpain [5,13] and elevated calpain activity accompanies phagocytosis and spreading [14, 15, 16, 17]. It is therefore significant that ezrin, which is a substrate for calpain, has been shown to be cleaved during phagocytic pseudopod extension [18,19]. This evidence has led to the proposal that the cell surface topography of neutrophils is important in providing a reservoir of membrane which is required for cell spreading and phagocytosis [2,3]. This hypothesis has been previously difficult to test directly. However, advances in monitoring cell surface topography in living cells using sdFRAP [20] have enabled the effects of experimental manipulations of cell surface topography and cell behaviour to be monitored and so test the hypothesis. Subdomain fluorescence recovery after

photobleaching FRAP (sdFRAP) involves measurement of the kinetics of fluorescence recovery at a locus remote from the bleach front. By comparison with the kinetics expected from a flat surface, the wrinkledness of the diffusion path can be established [20]. This approach can be done in real time and the effect of experimental manipulations determined on the individual cells under examination.

In this paper, it is shown that osmotic shrinking of neutrophils produces hyperwrinkled cells which fail to spread normally or undertake phagocytosis. By timing the osmotic jump to induce hyperwrinkling after the  $\text{Ca}^{2+}$  signalling and also by forcing  $\text{Ca}^{2+}$  signals by uncaging cytosolic  $\text{IP}_3$ , it was shown that the inhibitory effects of hyperwrinkling was attributed to the inability of  $\text{Ca}^{2+}$  signalling to release the osmotically induced wrinkles. The data in this paper therefore provides new evidence that the neutrophil surface topography provides the membrane reservoir for the large apparent increases in cell surface area which are necessary for phagocytosis and spreading by these cells.

## **Methods and Materials**

### **Materials**

DiI (1,1'-Dihexadecyl-3,3,3',3'-tetramethylindocarbocyanine perchlorate) was purchased from ThermoFisher Scientific; caged- $\text{Ins}(1,4,5)\text{P}_3$  /PM (D-23-O-Isopropylidene-6-O-(2-nitro-4,5-dimethoxy)benzyl-myo-Inositol 145-trisphosphate-Hexakis(propionoxymethyl) ester from Alexis Biochemical, U.S.A.; fluo4-acetoxymethyl ester from Molecular Probes Invitrogen, U.S.A; and all other reagents from Aldrich-Sigma.

### **Neutrophil preparation and osmolarity shifting**

Neutrophils were isolated from human blood taken from healthy volunteers with informed consent under Ethics Approval SMREC 10/01 (Cardiff University), and suspended in Krebs

medium (120 mM NaCl, 4.9 mM KCl 1.2 mM KH<sub>2</sub>PO<sub>4</sub>, 1.2 mM MgSO<sub>4</sub>, 1.3 mM CaCl<sub>2</sub>, 25 mM HEPES and 0.1% BSA, adjusted to pH 7.4 with NaOH as previously described [13]. Neutrophils were allowed to sediment onto a glass coverslip for observation by confocal microscopy at 37 °C. Care was taken to avoid inadvertent activation of the cells, which can occur during shaking or vigorous re-suspension. The cell suspension was kept on ice (4°C) before experimentation, and allowed to warm slowly to the required temperature (usually 37°C or 25°C) before the start of the experiment. During the experiment, at the required time, the osmolarity was shifted by the addition of the appropriate volume of warmed Krebs medium containing additional NaCl or sucrose, so that the osmolarity in the medium changed to a new value as a step function, whilst the cells were under observation. The concentrations of other ions in the extracellular environment, including Ca<sup>2+</sup>, were thus unaltered. Isotonicity was restored, when required, by the addition of the appropriate volume of Krebs medium without NaCl or sucrose, so that again the concentrations of other ions in the extracellular environment, including Ca<sup>2+</sup>, were again not changed during the osmolarity shift.

### **Cell and Ca<sup>2+</sup> imaging and IP<sub>3</sub> uncaging**

Cytosolic free Ca<sup>2+</sup> was measured as described in detail elsewhere [21] using the resonant scanning head of the Leica RS confocal microscope, which had a frequency of ~40 MHz on a thermostatically controlled stage (37±0.1°C). During image acquisition, uncaging of IP<sub>3</sub> was achieved by activating a 405nm diode laser, whilst alternate line-by-line imaging both the transmitted light (phase contrast) and emitted fluorescence excited by the 488nm laser. Using a cytosolic indicator of UV irradiation [22], it was shown that this procedure generated photolytic product linearly with no initial time delay and released IP<sub>3</sub> at a rate of about 4 μM/second [5].

### **Topography measurement by sFRAP and SEM**

Neutrophils were stained with, DiIC<sub>16</sub>(3), dissolved in DMSO (10mg/ml) by dilution (to 2μM) from the stock solution in cell suspension. After 120s, the excess DiIC<sub>16</sub>(3) was removed from adherent cells by washing, i.e. replacing the dye-containing extracellular medium with media at least 4 times. Confocal imaging (resonant scanning laser confocal microscope, Leica SP5) with low intensity excitation at 543nm to excite DiIC<sub>16</sub>(3) was begun and an argon laser line at 488nm activated for photo-bleaching. The emitted light was collected for imaging at 600–700nm. All experiments were performed at 37°C. The bleaching pulse was restricted to a defined region of the cell to produce a bleached zone at the membrane. The return of fluorescence to a defined subdomain in the bleached zone was recorded. The recovery of fluorescence was allowed to continue until a new equilibrium signal ( $F_{\max}$ ) was achieved. As the initial bleach reduces whole cell fluorescence, it was important to take this into account when estimating recovery [23]. Subdomains were measurement regions within the bleach zone (100nm×100nm), usually taken 1-2μm from the bleach front as previously described [20]. Diffusion of dye from the bleach front is described by  $D \propto x^2/\tau$ , where  $\tau$  is the characteristic time and  $x$  is the distance travelled. The linear wrinkledness of the path length (ie actual 2D travel/apparent 1D travel) is given by  $\sqrt{(\tau_{(w)})/(\tau_{(s)})}$  and the wrinkleness of the surface area ( $w$ ) is thus proportional to  $(\tau_{(w)})/(\tau_{(s)})$ . A smooth surface has  $w=1$  and wrinkled surfaces have  $w>1$ . More details are given in the appendix to ref 20. For scanning electron microscopy, neutrophils were fixed in suspension with glutaraldehyde (4% overnight) and then filtered on to porous membranes to produce a stable population of fixed cells for dehydration and sputter coating with gold. Scanning electron microscopy imaging was undertaken using a JEOL 840A scanning electron microscope (Joel UK, Hertfordshire, UK) within the Electronic Microscopy Unit of Cardiff University Medical School, operated by Dr Chris von Ruhland.

### **Cell spreading quantitation**

Neutrophils in suspension were allowed to sediment on to a glass coverslip of a modified counting chamber of an automated cell counter (Cellometer®: Peqab Ltd., Fareham, UK) before insertion into the machine, which acquires microscopic images from random areas of the slides for automated cell counting. The size thresholds used by the image analysis algorithm were set to distinguish “cells” from noise or debris ( $<7\mu\text{m}$ ) and also to count only small non-spread neutrophils ( $\text{diam} < 11\mu\text{m}$ ) and larger spread neutrophils ( $11\mu\text{m}$ ). These cut-off values were chosen, from knowledge of the initial cell size distribution, to divide the non-spread cell population into two approximately equal parts. Images and cell counting (in real time) were acquired at intervals over an extended period. This method measured more than 500 cell diameters/time point. The data are described as mean  $\pm$  S.E.M. Single neutrophil spreading measurements were made on individual neutrophils allowed to sediment onto glass coverslips at  $37^\circ\text{C}$  whilst acquiring an image sequence so that the complete spreading event from initial contact to maximum spread size was recorded for each cell. The areas of the cell during the time sequence were measured using Image J in-built software.

### **Cell movement analysis**

Random pseudopodia projections during random kinesis were quantified using the “tracking plug-in” (by Fabrice P. Cordelières) for Image J 1.52a (NIH, USA) and the membrane movement between consecutive “frames” recorded. The extension of phagocytic pseudopodia around the target was measured using the “free hand” function inbuilt in Image J to track the phagocytic cup size at 1-5sec intervals during internalisation.

### **Phagocytosis**

Zymosan particles (approx.  $2 \times 3 \mu\text{m}$  ovoids), opsonised by incubation with freshly prepared human serum at  $37^\circ\text{C}$  for 30mins, were added to neutrophils while observing microscopically. Contact between the neutrophils and the particles was allowed to occur by random chance and then followed as phagocytosis proceeded. In some experiments, opsonised zymosan particles were allowed to adhere to glass coverslips to give a coverage of adherent zymosan particles of about 1–2 zymosan particle/ $400\mu\text{m}^2$ . The neutrophils were allowed to sediment onto the zymosan-coated coverslip while observing microscopically, so that cells could be selected for experimentation which were close to adherent zymosan particles and so likely to undergo phagocytosis.

## **Results**

### ***Experimental manipulation of neutrophil surface topography***

Three experimental conditions, osmotic cell swelling, shrinking and amphiphilic plasma membrane expanders, have been explored. Using sdFRAP of DiI incorporated into the plasma membrane (fig 1a, b) to interrogate the cell surface topography [20], it was found that both chemical membrane expansion and hypertonic shrinking increased the degree of wrinkledness of the plasma membrane (tortuosity of the diffusion path). The wrinkle factor ( $w$ ) for DiI diffusion in the membrane increasing from  $w = 2.7 \pm 1.3$  to  $w = 4.3 \pm 0.71$  and  $w = 4.2 \pm 1.1$  ( $n=5$ ) for osmotic shrinkage and deoxycholate respectively (fig 1c). Hypo-osmotic swelling reduced the value of  $w$  to near unity (fig 1c), showing that the initially wrinkled surface of the neutrophil was almost flattened by osmotic swelling, but was made more wrinkled by chemical expansion or hypertonic shrinkage [20]. It was estimated from the decrease in cell volume induced by osmotic shrinkage, that the excess membrane accounted for the additional surface folds [20]. Scanning electron microscopy (SEM) of neutrophils also showed the increase in wrinkling associated with cell shrinking and that there were additional cell surface

features such as micro-bloating and bloated wrinkles on cells treated with membrane expanders (fig 1d). SEM also showed that the surfaces of osmotically swollen cells were not entirely smooth but retained some surface features (fig 1d). As these experimental approaches caused significant changes in the cell surface topography, the effect of these manipulations on the ability of neutrophils to undergo cell shape change was therefore examined.

### **Cell spreading and cell surface topography manipulation**

Hypo-osmotically swollen neutrophils, despite having an enlarged cell diameter in suspension, retained the ability to spread (fig 2,3). Osmotically swollen neutrophils were also able to undergo phagocytosis, but with a reduced capacity of 1.8 zymosan particles/cell in a 10 minute period compared to the capacity of normal neutrophils of 5.1 particles/cell. Two membrane expanders, deoxycholine and octanol, also had an effect on the ability of neutrophils to spread (fig 3b). Octanol slowed the approach to maximal spreading (fig 3b), but the final spread areas were similar to the untreated cells (fig 3b). In contrast, osmotic shrinking had a profound inhibitory effect on neutrophil spreading (fig 2,3). In hyperosmotic conditions, neutrophils failed to spread even after prolonged periods of contact with the adhesive surface (fig 3e). These effects were shown in both cell populations (fig 2 b,c) and at the individual cell level (fig 3c,d,e), where the final extent of spreading was similar to the untreated cells. It was concluded that osmotically hyperwrinkled cells (unlike cells with surface topographical modification induced by membrane expanders or hypo-osmotic swelling) were unable to undergo spreading.

The mechanism for this striking inhibitory effect of hyperosmolarity was therefore investigated. Trypan blue exclusion tests showed that there was no effect on crude cell viability (ie cell rupture), with greater than 95% of cells excluding trypan blue before and during osmotic shrinking, as well as after restoration to the iso-osmolarity (Suppl fig S1a) .

Furthermore, cell populations exposed to hyperosmotic conditions for 5 to 15 mins before restoring isotonicity in suspension, spread normally when allowed to sediment on to an adhesive surface (suppl fig S1c). This suggested that hyperosmotic treatment itself caused no major and irreversible damage to the cells. An important signal for neutrophil spreading is an elevation in cytosolic free  $\text{Ca}^{2+}$  [5, 24, 25]. This  $\text{Ca}^{2+}$  signal is triggered when a critical number of integrin molecules (or other adhesion molecules) are engaged [13]. Osmotically swollen neutrophils, those pre-treated with plasma membrane expanders or untreated all triggered a  $\text{Ca}^{2+}$  signal immediately before cell spreading (fig 4a,b). However, osmotically hyperwrinkled neutrophils failed to elicit this  $\text{Ca}^{2+}$  signal (fig 4c,d). Since this  $\text{Ca}^{2+}$  signal is triggered by  $\beta 2$  integrin engagement the osmotically hyperwrinkled cell surface may have physically prevented contact of integrin with the substrate. As, physiologically,  $\beta 2$  integrin is mainly located in the “valleys” between microridge/wrinkles [26, 27], osmotically induced extra wrinkles from membrane in this region may have  $\beta 2$  integrin. The  $\beta 2$  integrin on the surface of hyperwrinkled neutrophils may have not been coupled to the  $\text{Ca}^{2+}$  signal system or the topography of the cell surface may have prevented the engagement of a sufficient number of these integrin molecules to trigger the  $\text{Ca}^{2+}$  signalling.

Neutrophils were thus allowed to sediment onto the adhesive surface and begin receptor engagement until the point that the  $\text{Ca}^{2+}$  was triggered in isotonic conditions, before imposing the hyperosmotic condition (fig 4e,f). In this way, the effect of hyperwrinkling on cellular events after the  $\text{Ca}^{2+}$  signal could be studied. The immediate effect of hyperosmolarity in hyperwrinkling the cell was observed (fig 4c). There was also a temporary elevation of cytosolic  $\text{Ca}^{2+}$  (fig 4 e) which has been reported previously and may be due to reduction in cell volume. Cell spreading began within about 40 seconds of the  $\text{Ca}^{2+}$  signal (fig 4f), as seen in untreated cells (fig 4a). However, cell spreading by the now hyperwrinkled cell was asymmetrical with defined “pinch points” (indicated by arrows in fig 4c) where spreading

was restricted. This suggested the possibility that  $\text{Ca}^{2+}$ -sensitive wrinkles were released but that osmotically-induced wrinkles prevented full spreading.

In order to test this possibility, neutrophils were therefore loaded with caged  $\text{IP}_3$ , so that an  $\text{IP}_3$ -triggered  $\text{Ca}^{2+}$  signal could be produced by photolytic uncaging of  $\text{IP}_3$  within the cell. This approach has been used previously to cause  $\text{Ca}^{2+}$  signals in neutrophils and trigger an apparent plasma membrane expansion and spreading of neutrophils onto the substrate [5]. Unlike untreated cells, hyperwrinkled neutrophils did not immediately spread in response to the  $\text{Ca}^{2+}$  signal (fig 5a; supplementary data movie1). Instead, they produced small blebs which after a delay of 60-100s formed a significant membrane expansion in the form of elongated tubular blebs (fig 5a,c; supplementary data movie1). After the  $\text{IP}_3$  induced  $\text{Ca}^{2+}$  elevation in hyperwrinkled neutrophils, sFRAP showed that the topography of the cell body remained significantly wrinkled ( $w_{(\text{initial})}=4.3\pm 0.3$  reduced to  $w_{(\text{post } \text{Ca}^{2+} \text{ signal})}=3.1\pm 0.9$ ;  $n=4$ ), compared to the almost complete loss of wrinkledness (ie  $w_{(\text{smooth})}=1$ ) which occurred in untreated cells after the  $\text{Ca}^{2+}$  signal ( $w_{(\text{initial})}=2.6\pm 0.4$  to  $w_{(\text{post } \text{Ca}^{2+})}=1.43\pm 0.29$   $n=3$ ). This was consistent with the role of ezrin in maintaining cell surface wrinkles [10-12] and the signalling pathway from the  $\text{Ca}^{2+}$  signal to ezrin cleavage, as demonstrated previously [18,19]. It is proposed that the ezrin-maintained wrinkles were released, but that the osmotically formed wrinkles restrict membrane expansion to regions of the cell rather than the uniform membrane expansion seen with physiological cell spreading (fig 5d).

### **Cell surface topography affects cell motility**

Neutrophil spontaneous or chemo-kinesis requires membrane protrusions but, as with small membrane expansions, do not require  $\text{Ca}^{2+}$  signalling [4,28]. The role of cell surface topography was therefore investigated on this neutrophil behaviour as it avoided the complication of effects on  $\text{Ca}^{2+}$  signalling. Untreated neutrophils were therefore allowed to

adhere to the substrate and undergo spontaneous kinesis before the hypertonic challenge. Neutrophil kinesis was immediately halted by hyperosmotic conditions (fig 6; supplementary data movie 2), with similar effects of hyperosmolarity induced by either NaCl (fig 6b,e,g) or sucrose (fig 6d,e; movie 2). The cells are held in an immobilised state, with neither kinesis nor active membrane protrusions, for as long as they remain in hypertonic conditions (fig c,g; movie 2). This was consistent with the unavailability of osmotically formed wrinkles for cell shape changes. When isotonicity was restored, cell movement was gradually restored (fig 6g; movie 2). However, cell polarity was usually lost, and the cells formed pseudopodia symmetrically around the cell periphery (including perpendicularly to the plane of the substrate) rather than in a polarised fashion (fig 6 g,c,f). The upward thrust of the cells results in a retraction of the cell skirt is perhaps better seen dynamically after restoration of isotonicity at the end of supplementary movie 2. The loss of polarity and upward movement of the cell edge may be the result of the actin Brownian ratchet mechanism [29,30], which was initially restricted by the resistance of the plasma membrane. When additional membrane wrinkling was enforced by hyperosmolarity, the actin polymerisation would be prevented by the increased resistance of the plasma membrane; but when these osmotically-induced wrinkles were permitted to unfold by restoration of isotonicity, the actin Brownian ratchet was released and actin polymerisation resumed randomly at all available loci within the cell (fig 6 c,f).

### **Cell surface topography affects phagocytosis**

Phagocytosis, the key function of neutrophils, also requires a highly localised expansion of the membrane to form phagocytic pseudopodia, initially as a phagocytic cup and then by progression around the target particle to enclose the particle and form a phagosome. The effect of osmotic wrinkling on this process was thus investigated with the aim of testing the hypothesis that unwrinkling of the physiologically-maintained membrane reservoir is required

for completion of phagocytosis [2,18]. Phagocytosis of iC3b-opsomised zymosan particles was completely inhibited by osmotic hyperwrinkling (maximum zymosan internalisation: control cells= 9 particles/cell: hyperwrinkled cells= 0 particles/cell). However, it was anticipated that, as with cell spreading, the  $\text{Ca}^{2+}$  signal would be absent, as the wrinkled membrane would fail to present sufficient integrin molecules to trigger the signal. The phagocytic  $\text{Ca}^{2+}$  signal is triggered when approximately half the C3bi-opsomised zymosan particle is held within a phagocytic cup [13]. Experiments were therefore undertaken in which the hypertonic condition was imposed on the cell during phagocytosis, after the  $\text{Ca}^{2+}$  signal had been triggered but before completion of phagocytosis. It was found that, as with neutrophil kinesis, the imposition of hyperwrinkling immediately halted the progression of phagocytosis (n= 26: fig 7a,b). This indicated that the inhibitory action of hyperwrinkling was after the physiological  $\text{Ca}^{2+}$ -triggered release of ezrin maintained wrinkles. The restoration of isotonicity allowed neutrophil motility to resume (fig 7b,c). As with kinesis, membrane expansion resumed at random locations on the cell surface causing a retraction of the cell edge away from the phagocytic target. In 7 experiments however, the phagocytic cup remained (eg fig 7 and 8). However, in only 2 of these 7 examples, did restoration of isotonicity result in progression and completion of phagocytosis (fig 8). In the example shown in figure 8, the arrest of phagocytosis was maintained for 100 seconds at the phagocytic cup stage (fig 8a), but when isotonicity was restored, the progression of the phagocytic pseudopodia around the zymosan target resumed (fig 8a,b). The progression of phagocytosis, monitored by measurement of the size of the phagocytic cup as a fraction of the complete phagosome, showed that the rate of progression of the phagocytic pseudopodia around the zymosan particle after recovery from hyperosmotic arrest was almost equal to initial rate of the pre-hyperwrinkled cell (0.056  $\mu\text{m/s}$  and 0.064 $\mu\text{m/s}$  respectively). In contrast, during the hyperosmolar condition, the rate of progression of the pseudopodia

around the particle was almost zero ( $<0.002\mu\text{m/s}$ ). The result of restoration of isotonicity, on rare occasions, could thus be a “normal” completion of phagocytosis and internalisation of the zymosan particle within a phagosome. It is not clear why some cells were able to continue with phagocytosis, while the majority were not. However, the effect of osmotic reversal was to cause the cells to lose polarisation (see Supplementary fig S3) and as the cells push up and away from the substrate for the cell edges to retract. Both these events would withdraw the pseudopodia (forming the phagocytic cup) away from the phagocytic target. In the cells which were able to continue with phagocytosis, there were atypical “robust” extending pseudopodia (compare the cell shown in fig 7 and fig 8), which may have been better able to resist the retraction effect.

## **Discussion**

The data presented here is consistent with the wrinkled cell surface topography of neutrophils being the membrane reservoir and that, by unfolding, provides the increase in availability of membrane for cell spreading and phagocytosis by these cells. The requirement for unfolding of surface wrinkles and microridges has also been suggested by biophysical approaches, such as cortical tension monitoring by single cell micropipette aspiration [eg 4,8] and by whole cell capacitance measurement [6]. There is similar evidence emerging in other cell types including lymphocytes [31]. It is important to note that different cell types may respond differently. For example, in Ehrlich Lettre ascites cells, cytosolic ezrin translocates to wrinkles and protrusions formed by osmotic cell shrinkage [32] thus generating an ezrin-maintained membrane reservoir. Equivalent cortical cross-linking proteins have also been reported at the cortex of amoeba when hyper-osmotically shrunk [33]. In neutrophils, immunodetection of ezrin shows that there is little cytosolic ezrin [18 and supplementary figure S2] and that all

available ezrin is held at the cell cortex maintaining the membrane reservoir wrinkles before hyperosmotic challenge. During the “tubulation” induced by elevating cytosolic  $\text{Ca}^{2+}$ , as shown in figure 5, immunohistochemistry also shows a localised loss of ezrin from the cell cortex at the sites of initiation of tubular bleb formation (supplementary fig S2), before the global loss of cortical ezrin (fig S2), suggesting a connection between the two events.

Membrane tension is also known to be an important regulator of related phenomena [34]. Clearly, membrane tension and the firm holding of the wrinkles at the cell surface are closely related and thus osmotic and membrane expanding manipulations have been used in studies of membrane tension. Osmotic swelling has been shown to increase membrane tension, while chemical membrane expanders and osmotic shrinking both reduced cell surface tension. The membrane expander deoxycholate, reduces the membrane tension to 50% of normal [35] and hyperosmolarity reducing the tension in nematode sperm cells to 20% of normal [36]. Despite the similar effects on membrane tension, these manipulations had strikingly different effects on neutrophil phagocytosis and spreading. The membrane expanders had very little effect whereas, hyper-osmotic media totally inhibited the ability of neutrophils to change shape, even when  $\text{Ca}^{2+}$  signalling was allowed to occur before imposition of hyperwrinkling or  $\text{Ca}^{2+}$  signalling was forced by  $\text{IP}_3$  uncaging (figs 4,5,7,8). The difference in outcome of two manipulations which decrease membrane tension, may suggest an explanation other than membrane tension. The membrane expanders clearly increased the wrinkledness of the cell surface (fig 1), and probably added new surface area to the plasma membrane randomly. Thus wrinkles and microridges, as well as the valleys between them, may equally have an expanded membrane. Thus when signalled by  $\text{Ca}^{2+}$  to release the ezrin-held wrinkles, the resultant membrane expansion was little affected. In contrast, when the cells were in hyperosmotic conditions, the release of ezrin maintained wrinkles would not result in a totally unwrinkled cell surface, as osmotically induced wrinkles would remain. It is thought that in

many cell types, exocytosis is the membrane reservoir. In macrophage phagocytosis, both systems act at different points in time. Initial membrane unfolding provides the additional membrane and, once exhausted, exocytosis adds more membrane [7]. There is a wealth of evidence for the Sheetz hypothesis that high membrane tension favours exocytosis and recruits intracellularly-stored membrane to the surface; whereas low tensions favour endocytosis and retrieval of plasma membrane. Whole cell membrane capacitance measurements suggest membrane is added by exocytosis during osmotic swelling, and excess membrane is internalised during cell shrinking [37,38]. The lowered membrane tension in neutrophils induced by hyperosmolarity might therefore be expected to increase phagocytosis and other “membrane recovery” mechanisms, such as pinocytosis, rather than prevent it. While phagocytosis and cell spreading are thought of as similar phenomena, in terms of membrane recovery they are, of course very different; phagocytosis internalising membrane and cell spreading stretching out the membrane without recovery. However, we found that cell spreading was similarly inhibited by hyperosmotic conditions. Interestingly, during fibroblast spreading, the initial phase of spreading occurs without any additional surface area membrane, as with macrophage phagocytosis, and exocytosis is only detected later [39]. The inhibitory effects of hyperosmotic conditions on cell movement and cell shape change is not restricted to neutrophils. For example, hyperosmotic conditions, reduce *Xenopus* epidermal cell locomotion [40] and the formation of surface blebs on carcinosarcoma cells, together with cell locomotion and cell polarity were all prevented by hyperosmotic conditions [41]. In these latter cells, the reduction in shape change activity correlated with cell volume reduction (ie excess surface membrane folding) and not with changes in the F-actin content, which also occurred. The increase in f-actin during osmotic shrinking [42] especially at the cell cortex [43] has also been observed in neutrophils. This may be the result of the release of the Brownian ratchet restraint after hyperwrinkling allowing cortical actin polymerisation [29].

This would also explain the lack of cell polarity in neutrophils after the hyper-osmotic/isotonic recovery step observed here (fig 6: supplementary data movie 2).

Although the changes in osmolarity were used here purely as an experimental means of hyperwrinkling the neutrophil cell surface, the inhibition of adhesion and phagocytosis in these conditions may have some clinical implications. Neutrophils experience high osmolarities in the urinary tract, as high as 1400mOsM in the renal medulla [44]. The inhibition of neutrophil phagocytosis of microbes here may contribute to local infection at this site. In many inflammatory sites, especially with cysts or other enclosed spaces, the osmolarity can rise to high levels, due to hydrolysis of macromolecules into smaller (osmotically active) molecules [45] which may have an impact of the ability of neutrophils to function efficiently. Clinically, hyperosmotic resuscitation fluids, which are often used to restore circulating volume in the hypovolemic patients, may have unwanted or even beneficial immunosuppressive effects. It has been suggested that hyperosmotic perfusion fluid may be useful in inhibiting neutrophil-mediated organ injury [46].

From the work presented here, it is concluded that the wrinkled neutrophil surface topography provides the rapidly-accessed membrane reservoir required by these cells for phagocytosis and cell spreading. Since neutrophils are the cell type *par excellence* able to perform both these functions, with speed and high phagocytic capacity, it could be argued they are tuned to use this approach over the slower and more energy expensive exocytosis and endocytosis mechanism which other cell types may use. In neutrophils, at least, the control of exo/endocytosis by membrane tension itself seems to play very little part in the rapid cell shape changes that these cells undertake and, in these cells, the plasma membrane reservoir is the plasma membrane itself.

## **Declaration of interest**

The authors declare no competing or financial interests.

## **Author contributions**

Aljumaa: Investigation, Methodology, Validation, Writing- Original draft preparation. Hallett & Dewitt: Conceptualization, Methodology, Formal analysis, Supervision, Data Curation, Writing- Reviewing and Editing

## **Funding**

This work was funded by the Saudi Arabian Cultural Bureau (SACB) [grant number 1027765195]. The funder had no role in the collection, analysis and interpretation of data.

## References

- [1] Herant M, Heinrich V, Dembo M. (2006) Mechanics of neutrophil phagocytosis: experiments and quantitative models. **J. Cell Sci.** 19:1903–1913.
- [2] Hallett, M.B., Dewitt, S. (2007) Ironing out the wrinkles of neutrophil phagocytosis. **Trends Cell Biol.** 17: 209-214
- [3] Dewitt, S., Hallett, M.B. (2007) Leukocyte membrane "expansion": a central mechanism for leukocyte extravasation. **J. Leuk. Biol.** 81: 1160-1164
- [4] Francis, E.A., Heinrich, V. (2018) Extension of chemotactic pseudopods by nonadherent human neutrophils does not require or cause calcium bursts. **Science Sig.** 11 Art Num: eaal4289. DOI: 10.1126/scisignal.aal4289
- [5] Dewitt, S., Francis, R.J., Hallett, M.B. (2013) Ca<sup>2+</sup> and calpain control membrane expansion during the rapid cell spreading of neutrophils. **J. Cell Sci.** 126:4627-463
- [6] Di, A., Krupa, B., Bindokas, V.P., Chen, Y., Brown, M.E., Palfrey, H.C., Naren, A.P., Kirk, K.L., Nelson, D.J. (2002) Quantal release of free radicals during exocytosis of phagosomes. **Nature Cell Biol.** 4, 279–285
- [7] Masters, T.A, Pontes, B., Viasnoff, V., Li, Y., Gauthier, N.C. (2013) Plasma membrane tension orchestrates membrane trafficking, cytoskeletal remodeling, and biochemical signaling during phagocytosis **Proc Natl. Acad. Sci (USA)** 110, 11875-11881
- [8] Herant, M., Heinrich, V. Dembo, M. (2005) Mechanics of neutrophil phagocytosis: behavior of the cortical tension. **J Cell Sci** 118: 1789-1797
- [9] Francis, E.A., Heinrich, V. (2018) Mechanistic understanding of single-cell behavior is essential for transformative advances in Biomedicine. **Yale J. Biol. Med.** 91, 279–289
- [10] Algrain, M., Turunen, O., Vaheri, A., Louvard, D., Arpin, M. (1993) Ezrin contains cytoskeleton and membrane binding domains accounting for its proposed role as a membrane-cytoskeletal linker. **J. Cell Biol.** 120, 129–139.
- [11] Yonemura, S., Tsukita, S., Tsukita, S. (1999) Direct involvement of ezrin/radixin/moesin (ERM)-binding membrane proteins in the organization of microvilli in collaboration with activated ERM proteins. **J. Cell Biol.** 145, 1497–1509
- [12] Rouven Brückner, B. Pietuch, A., Nehls, S., Rother, J., Janshoff, A. (2015). Ezrin is a major regulator of membrane tension in epithelial cells. **Sci. Rep.** 5, 14700; doi: 10.1038/srep14700.

- [13] Dewitt S., Hallett M.B. (2002) Cytosolic free  $\text{Ca}^{2+}$  changes and calpain activation are required for beta integrin-accelerated phagocytosis by human neutrophils. *J. Cell Biol.* 159, 181-189
- [14] Dewitt S., Laffafian, I., Hallett M.,B. (2003) Phagosomal oxidative activity during beta 2 integrin (CR3)-mediated phagocytosis by neutrophils is triggered by a non-restricted  $\text{Ca}^{2+}$  signal:  $\text{Ca}^{2+}$  controls time not space. *J. Cell Sci.* 116, 2857-2865
- [15] Lewis, K.J., Masterman, B., Laffafian, I., Dewitt, S., Campbell, J.S., Hallett, M.B. (2014) Minimal impact electro-injection of cells undergoing dynamic shape change reveals calpain activation. *Biochim. Biophys. Acta –Mol. Cell Res.* 1843, 1182-1187
- [16] Campbell, J.S., Hallett, M.B. (2015) Active calpain in phagocytically competent human neutrophils: Electroinjection of fluorogenic calpain substrate. *Biochem. Biophys. Res. Commun.* 457, 341-346
- [17] Jennings, S., Hallett, M.B. (2019) Single cell measurement of calpain activity in neutrophils reveals link to cytosolic  $\text{Ca}^{2+}$  elevation and individual phagocytotic events. *Biochem. Biophys. Res. Commun.* 515, 163-168
- [18] Roberts, R.E., Hallett M.B. (2019) Neutrophil cell shape change: Mechanism and signalling during cell spreading and phagocytosis. *Int. J. Mol. Sci.* 19, 1383 -1398
- [19] Roberts RE, Martin M, Marion S, Elumalai GL, Lewis K, Hallett MB. (2020)  $\text{Ca}^{2+}$ -activated cleavage of ezrin visualised dynamically in living myeloid cells during cell surface area expansion. *J Cell Sci.* 133(5) doi: 10.1242/jcs.236968
- [20] Al Jumaa, M. A., Dewitt, S., Hallett, M.B. (2017) Topographical interrogation of the living cell surface reveals its role in rapid cell shape changes during phagocytosis and spreading. *Sci. Rep.* 7, Article Number: 9790
- [21] Hillson, E.J., Hallett M.B. (2007) Localised and rapid  $\text{Ca}^{2+}$  micro-events in human neutrophils: Conventional  $\text{Ca}^{2+}$  puffs and global waves without peripheral-restriction or wave cycling. *Cell Calcium* 41, 525-536
- [22] Brasen J.C., Dewitt, S., Hallett M.B. (2010) A reporter of UV intensity delivered to the cytosol during photolytic uncaging. *Biophys J.* 98, L25-L27
- [23] Hardy, L. R. (2012) Fluorescence recovery after photobleaching (FRAP) with a focus on f-actin. *Curr Protoc Neurosci.* 61, 2.17.1-2.17.12
- [24] Kruskal, B.A., Shak, S., Maxfield F.R. (1986) Spreading of human neutrophils is immediately preceded by a large increase in cytoplasmic free calcium. *Proc. Natl. Acad. Sci. U. S. A.* 83, 2919-2923

- [25] Pettit, E.J. and Hallett M.B. (1996) Localised and global cytosolic  $Ca^{2+}$  changes in neutrophils during engagement of CD11b/CD18 integrin visualised using confocal laser scanning reconstruction. **J. Cell Sci.** 109, 1689-1694.
- [26] Erlandsen, S. L., Hasslen, S.R., Nelson, R.D. (1993) Detection and spatial distribution of the  $\beta 2$  integrin (Mac-1) and L-selectin (LECAM1) adherence receptors on human neutrophils by high-resolution field emission SEM. **J. Histochem. Cytochem.** 41, 327–333.
- [27] Lomakina, E.B., Marsh, G., Waugh R.E. (2014) Cell surface topography is a regulator of molecular interactions during chemokine-induced neutrophil spreading. **Biophys. J.** 107. 1302-1312
- [28] Laffafian I and Hallett M.B., (1995) Does cytosolic free  $Ca^{2+}$  signal neutrophil chemotaxis in response to formylated chemotactic peptide. **J. Cell Sci.** 108; 3199-3205
- [29] Peskin, C.S., Odell, G.M., Oster, G.F. (1993) Cellular motions and thermal fluctuations: The Brownian ratchet. **Biophys. J.** 65, 316–324
- [30] Mogilner, A., Oster, G.. (1996) The physics of lamellipodial protrusion. **Eur Biophys J. Biophys.** 25 47-53
- [31] Guillou L., Babataheri A., Saitakis M., Bohineust A., Dogniaux S., Hivroz C., Barakat Al., Husson J. (2016) T-lymphocyte passive deformation is controlled by unfolding of membrane surface reservoirs. **Mol Biol Cell.** 27, 3574-3582.
- [32] Rasmussen, M., Alexander, R.T., Darborg, B.V., Møbjerg, N., Hoffmann, E.K., Kapus, A., Pedersen, S.F. (2008) Osmotic cell shrinkage activates ezrin/radixin/moesin (ERM) proteins: activation mechanisms and physiological implications. **Am. J. Physiol. Cell. Physiol** 294, C197–C212
- [33] Zischka H., Oehme F., Pintsch T., Ott A., Keller H., Kellermann J., Schuster S.C. (1999) Rearrangement of cortex proteins constitutes an osmoprotective mechanism in Dictyostelium. **EMBO J.** 18, 4241-4249
- [34] Diz-Munoz, A., Fletcher, D. A., Weiner, O.D. (2013) Use the force: membrane tension as an organizer of cell shape and motility. **Trends Cell Biol.** 23, 47-53
- [35] Raucher, D., Sheetz MP. (2000) Cell Spreading and Lamellipodial Extension Rate Is Regulated by Membrane Tension. **J Cell Biol.** 148: 127–136.
- [36] Batchelder EL, Hollopeter G, Campillo C, Mezanges X, Jorgensen EM, Nassoy P, Sens P, Plastino J. (2011) Membrane tension regulates motility by controlling lamellipodium organization. *Proc Natl Acad Sci U S A.* 12;108(28):11429-34.
- [37] Sukhorukov VL, Arnold WM, Zimmermann U (1993) Hypotonically induced changes in the plasma membrane of cultured mammalian cells. **J Membr. Biol.** 132, 27–40

- [38] Wan X., Harris J.A., Morris C.E. (1995) Responses of neurons to extreme osmotic stress. **J. Membr. Biol.** 145:21–31
- [39] Gauthier, N.C. Fardin, M.A., Roca-Cusachs, P., Sheetz, M.P. (2011) Temporary increase in plasma membrane tension coordinates the activation of exocytosis and contraction during cell spreading. *Proc. Natl. Acad. Sci. (USA)* **108**, 14467-14472
- [40] Strohmeier R., Bereiter-Hahn J. (1987) Hydrostatic pressure in epidermal cells is dependent on Ca-mediated contractions. **J Cell Sci.** 88, 631-640
- [41] Fedier A, Keller HU (1997) Suppression of bleb formation, locomotion, and polarity of Walker carcinosarcoma cells by hypertonic media correlates with cell volume reduction but not with changes in the Ehrlich content. **Cell Motil Cytoskeleton** 37, 326–337.
- [42] Rizoli S.B., Rotstein, O.D., Parodo J., Phillips. M.J., Kapus, A. (2000) Hypertonic inhibition of exocytosis in neutrophils: central role for osmotic actin skeleton remodelling. **Am. J. Physiol. - Cell Physiol.** 279, C619-C633
- [43] Ciano, C.D., Nie, Z., Szász, K., Lewis, A., Uruno, T., Zhang, X., Rotstein, O.D., Mak, A., Kapus, A. (2002) Osmotic stress-induced remodeling of the cortical cytoskeleton. **Am. J. Physiol. - Cell Physiol.** 283, C850-C865
- [44] Bryant RE, Sutcliffe MC, McGee ZA. (1972) Effect of osmolarities comparable to those of the renal medulla on function of human polymorph nuclear leukocytes. **J. Infect. Dis** 126, 1-10.
- [45] Leak, L.V. and J.F. Burke. (1974) Early events of tissue injury and the role of the lymphatic system in early inflammation, in: B.W. Zweifach, L. Grant, R.T. McCluskey (Eds.), **The Inflammatory Process**, Academic Press, New York/London.
- [46] Rizoli S.B., Kapus A., Fan J., Li Y.H., Marshall J.C., Rotstein O.D. (1998) Immunomodulatory effects of hypertonic resuscitation on the development of lung inflammation following hemorrhagic shock. **J. Immunol.** 161, 6288-6296

## Figure Legends

### Figure 1. Cell surface topography changes detected by sdFRAP and SEM

(a) The principle of subdomain fluorescence recovery after photobleaching (sdFRAP) is shown in the illustration. The kinetics of increase in diI fluorescence in the subdomain within the bleached area depends on the diffusion distance (illustrated by the dotted arrow). By comparing the kinetics expected from a flat surface with that actually recorded, the degree of surface wrinkledness can be estimated. (b) The subdomain fluorescence recovery time course, data from an experiment in which the membrane is fully flattened (ie smooth). The fluorescence intensity change within the subdomain over time, is given as a fraction of the maximum recovery ( $F/F_{\max}$ ). The wrinkled value ( $w$ ) was unity. (c) Typical sdFRAP recordings of the surfaces of neutrophils treated as indicated. The measured characteristic recovery time ( $\tau$ ) and the calculated wrinkled factor ( $w$ ) are shown. (d) Scanning electron micrographs showing the cell surfaces of neutrophil as indicated. Hypotonic (50% isotonicity), hypertonic (isotonic plus 300mOsM NaCl) and “DOC” (deoxycholate, 0.4mM).

### Figure 2. The effect of osmolarity on spreading diameters of neutrophil populations.

(a) shows the distribution of neutrophil diameters of neutrophils in the cell population before spreading, recorded by an automatic cell counter. The arrow indicates that the 11 $\mu$ m cut-off values used in the subsequent analysis, approximately divides the initial population in to two equal parts. This allows both in an increase in cell diameter (ie with spreading and with osmotic swelling) and a decrease in cell diameter (as with osmotic shrinking) to be recorded. (b) The changes in the ratio of cells having diameters greater than and less than the cut-off value is shown over time. An increase in the ratio indicates that there are more cells in the population which have spread on the imaging surface. The initial ratio reflects the effect of the different osmotic conditions on cell diameter of cells in suspension. (c) The percentage of cells in the population having greater than and less than the cut-off value is shown for three conditions, iso-osmotic, hypo-osmotic (50% isotonicity) and hyperosmotic (plus 300mOsM). More than 200 cell diameters were measured at each time point. The error bars in (b) show the mean  $\pm$  sem of  $N(>11\mu\text{m})/N(<11\mu\text{m})$ , the ratio of the number of cells have diameters greater or less than 11 $\mu$ m (vertical) and the time range over which the measurements were made (horizontal).

### Figure 3. The effect of osmolarity and membrane expanders on individual neutrophil spreading parameters

(a) The cell areas were measured on first contact with the imaging surface (initial) and also 20 mins later (final). The bars shows the mean  $\pm$  sem of neutrophil areas without osmotic

manipulation (iso-osmotic, n = 9); in hypo-osmotic medium (150mOsM, n = 10); and in hyperosmotic media (600mOsM, n = 10). There were significant differences between the initial and final cell areas for the neutrophils in iso-osmotic and hypo-osmotic media but not for hyperosmotic conditions. (b) The initial and final area of spreading cells was measured following pretreatment of the cells for 15 mins with deoxycholate, 0.4mM (DOC), octanol (0.4mM) or 15 min sham preincubation (control) and is shown, together with the time taken to achieve the final spread area. The vertical axis shows the cell area ( $\mu\text{m}^2$ ) for the first two histogram blocks, and time (s) for the last histogram block as indicated. The mean and sd for each condition is shown where n = 8 for deoxycholate, n = 9 for octanol and n = 8 for control. There was no significant difference in contact area either before or after spreading. Octanol treated cells took significantly longer to spread than either control or deoxycholate treated cells ( $p < 0.05$ , t-test). (c, d and e) shows the effect on spreading of osmotically treated neutrophils. (c) Shows two untreated neutrophils at first contact with the glass coverslip, and 48s later when spreading was complete. (d) shows two osmotically swollen spherical neutrophils, at first contact with the glass coverslip and 3 mins later when both cells have spread fully. During the interval, another spherical neutrophil sedimented into the imaging area indicated by asterisk. (e) Shows initially one osmotically shrunk neutrophil at first contact with the glass coverslip which is accompanied by another at 3 mins (indicated by the asterisk). The more wrinkled morphology of these cells may be apparent in the phase contrast images. No cells spread during the 25 mins recording period. These results were typical of at least 12 other experiments with neutrophils from four different donors.

#### **Figure 4. $\text{Ca}^{2+}$ signalling and hyper-wrinkled neutrophil spreading**

(a) The upper series of images show the phase contrast images (PC) with corresponding fluo4 intensity images ( $\text{Ca}^{2+}$ ) at the times indicated. In this example, a pair of cells was chosen to illustrate the relationship of an elevation in cytosolic  $\text{Ca}^{2+}$  and subsequent rapid spreading (by the cell arrowed). The cell which failed to generate a  $\text{Ca}^{2+}$  signal did not subsequently spread. (b) shows the time course of the fluo4 intensity changes in the spreading cell as relative intensity ( $F/F_{\text{max}}$ ) as a monitor of cytosolic  $\text{Ca}^{2+}$ . This experiment was typical of many similar obtained in at least three other donors. (c) The image pairs show osmotically hyperwrinkled neutrophils (600mOsM) which failed to spread and (d) show the accompanying failure to signal  $\text{Ca}^{2+}$ . (e and f) shows a typical experiment in which untreated neutrophils were allowed to sediment into the imaging plane and immediately after signalling  $\text{Ca}^{2+}$ , the osmolarity was increased by 300mOsM as indicated by the arrows in the  $\text{Ca}^{2+}$  trace in (e) and the image sequence (f). (f) The upper sequence of images shows the phase contrast images (PC) and the lower the fluo 4 signal ( $\text{Ca}^{2+}$ ). The immediate effect of hyperosmolarity in wrinkling the cell may be seen in the first image after the increase in osmolarity (36s), and the effect on spreading seen at the end of the sequence, where an asymmetric spreading with defined “pinch points” (indicated by arrows in the final image) where spreading is restricted. The complete  $\text{Ca}^{2+}$  signal and the timing of the hypertonic step for this experiment is shown in (e). This experiment was typical of four others from four different blood donors.

### **Figure 5. Effect of induced $\text{Ca}^{2+}$ signal by $\text{IP}_3$ uncaging on hyper-wrinkled cells**

Hyper-wrinkled neutrophils were induced and maintained by hyperosmotic medium during the course of the experiment. (a) Shows a typical experiment in which a  $\text{Ca}^{2+}$  signal was induced in osmotically wrinkled neutrophils preloaded with caged  $\text{IP}_3$ . The upper sequence of images shows the fluo4 intensity to monitor cytosolic  $\text{Ca}^{2+}$  (labelled  $\text{Ca}^{2+}$ ); and the lower sequence show the corresponding phase contrast images (PC) at the time shown. The timing of the  $\text{IP}_3$  uncaging pulse is shown in the sequence. (b) The complete time course for fluo4 intensity change (cytosolic  $\text{Ca}^{2+}$  signal) in the hyperwrinkled cell (upper trace) and the 405nm laser uncaging pulse (lower trace) are shown. (c) shows an enlarged image of the final stage of the cell with extended tubular blebs. This experiment was typical of three other experiments performed on cells from different donors and is shown in full in the supplementary data (movie 1). (d) The cartoon shows the possible mechanism. On the left is shown the initial state with some cell surface wrinkles being held by membrane cytoskeletal proteins which are physiologically releasable by a  $\text{Ca}^{2+}$  influx signal; and other wrinkles the result of osmotic shrinkage of the cell. On the right is shown the situation after the  $\text{Ca}^{2+}$  signal, where the physiological wrinkles are released as the cross-linking proteins, such as ezrin are cleaved, but the osmotic wrinkles remain in place and restrict the membrane expansion to small regions of the cell surface which consequently have large blebs. The same mechanism may underlie the effect (shown in fig 4c) when a physiological  $\text{Ca}^{2+}$  produces limited cell spreading after hyperwrinkling is induced. Presumably in this latter situation, many of the ezrin-maintained wrinkles have begun to unfold before the osmotic wrinkles have formed, and so spreading is restricted by “pinch points” at loci where osmotic wrinkling has occurred.

### **Figure 6. The effect of hyper-osmolarity on neutrophil kinesis**

(a-f) Frames from a continuous “movie” are shown to demonstrate the arrest of spontaneous kinesis by neutrophils subjected to a hyperosmotic step up (300mOsM to 600mOsM) using NaCl (a-c) or sucrose (d-f) to increase the osmolarity by 300mOsM. Images (a) and (d) show a single frame of the cells in isotonic medium. The cell movement is in best seen in the movie 2 (Suppl data) from which the frame was taken. Images (b) and (e) show the cells stationary in hyperosmotic medium. This is again best seen in the movie where the initial cell movement and stasis can be more easily seen. Images (c) and (f) show the effect of restoring isotonicity. This experiment was typical of those performed on at least 5 occasions. (g) The movement of a single neutrophil is quantified as movement of protrusion per frame ( $D(\text{position})/dt$ ) and the cumulative effect of these movements ( $\Sigma$  (pseudopod movement)). The data for this figure is also shown in the supplementary data (movie 2) as the complete sequence.

### **Figure 7. Arrest of phagocytosis by hyperwrinkling**

The figure shows a typical experiment in which phagocytosis is arrested after a  $\text{Ca}^{2+}$  signal has been triggered by phagocytic cup formation, by an hyperosmotic step. (a) shows a sequence of images with an opsonised zymosan particle (labelled  $Z^*$ ), the phagocytic neutrophil (labelled C1) and another non-phagocytic lymphocyte to act as a sentinel for the osmotic change (labelled C2). At the times shown, the images show the cell before contact (0s), at contact (20s) and at phagocytic cup formation and  $\text{Ca}^{2+}$  signalling (79 s). At this point, the osmolarity was stepped up by 300mOsM. The effect of the hyperosmolarity is clearly seen on the sentinel cell (C2) in the next image (at 81 s). Subsequent images shown that phagocytosis ceases to progress. The complete data set for this experiment is shown in the supplementary data (movie 3). (b) The movement of the neutrophils is quantified as movement of protrusion per frame ( $D(\text{position})/dt$ ) and the cumulative effect of these movements ( $\Sigma$  (pseudopod movement)). Although cell movement is restored by isotonicity, the cell fails to complete phagocytosis as shown in (fig 7a). (c) shows the accompanying cytosolic  $\text{Ca}^{2+}$  time course and the osmolarity step in relation to the  $\text{Ca}^{2+}$  signal. Similar results were obtained in similar experiments with neutrophils from three other donors on different days.

### **Figure 8. Arrest and recovery of phagocytosis by hyperwrinkling**

Completion of phagocytosis by hyperwrinkled neutrophils by restoration of isotonicity was found in only 2 out of 7 attempts. In the example here, as shown in (a), the progression of phagocytosis was monitored by measurement of the size of the phagocytic cup as a fraction of the complete phagosome. The rate of progression of the phagocytic pseudopodia around the zymosan particle after recovery from hyperosmotic arrest was almost equal to initial rate the by the untreated cell. During hyperosmolar conditions, the rate of progression of the pseudopodia around the particle was almost zero. (b) shows images taken from the complete sequence at the times indicated. The first 2 images show the initial stages of phagocytosis in isotonic conditions. The shaded arrow indicates the change in osmolarity from isotonicity to hyperosmolarity. The images at 100s and 200s are during the hyperosmotic conditions. The reverse-shaded arrow represents to return of osmolarity to isotonic. The last images show the quick completion of the phagocytic event begun before the hyperosmotic interlude and also the progression to phagocytosis of near-by particles.

## Supplementary Material - Figure Legends

**Fig S1 Experimental modification of neutrophil membrane topography: Viability of cells.** Cell viability as assessed by (a) trypan blue exclusion (%TP exclusion) in 2 separate experiments, (b) resting cytosolic  $\text{Ca}^{2+}$  concentration, assessed by fluo4 intensity (n=20 cells) and (c) cell spreading, assessed by the area of the cell presents at time zero (at first contact with the substrate) and 25 mins later (25'). In all parts of the figure, the label "iso" indicates the data for cells in isotonic medium; "hyper" the data for cells in hypertonic medium; "hypo" the data for cells in hypotonic medium and "DOC" indicates cell pretreated with deoxycholate. (a) shows the data for the restoration of isotonicity after hypertonic or hypotonic medium of cells in suspension before retesting the spreading ability marked as "+" for the osmotic condition indicated and then "iso" for the same cells after restoration of isotonicity. (c) the spreading by the cells from the same populations of cells in isotonic (iso) hypertonic conditions (hyper: 25 mins) and then and after restoration of isotonicity (hyper/iso) before re-testing their spreading ability.

**Figure S2 Ezrin distribution in hyperwrinkled neutrophils during tubular bleb formation.** The distribution of ezrin was visualised by histochemistry of fixed cells (details in ref 18) where (a) shows the typical cortical distribution in spherical (hyperwrinkled, non spreading) cells with possible surface wrinkles indicated; (b) a shows a typical tubulated cell (outlined in the white dotted line, with the tubular blebs indicated by asterisks) with no cortical ezrin detected; (c) shows a cell with a single tubular bleb forming as shown in the cell outline (white dotted line); (d) the corresponding ezrin distribution; (e) shows the cell outline superimposed onto the ezrin distribution where the localised loss of ezrin is indicated by the arrows.

**Fig S3 Loss of polarity and directionality after restoration of isotonicity to**

**hyperwrinkled neutrophils undergoing chemokinesis.** (a) Polarity was quantified as the ratio of the major axis (x) to the minor axis (y) as indicated in the image of a cell arrested in hypertonic medium (marked “H”) and the same cell after restoration of isotonicity (marked “R”). The data show the mean and SD of the polarity measurement from 14 cells in 3 separate experiments. (b) shows the movement of the cell edge of a neutrophil undergoing chemokinesis during the hypertonic and isotonicity restoration. The data shows the changing location of the cell edge as the distance from its final location at the times indicated, Dist (t) as a fraction of the maximum distance travel ( $\text{dist}_{\text{max}}$ ). The data, from a single representative cell, shows (i) the movement of the cell edge away from its final locus in isotonic medium, (ii) the arrest of movement during hypertonic hyper-wrinkling and (iii) the retraction of the cell edge towards its final location on restoration of isotonicity.

### **Movie 1: Effect of induced $\text{Ca}^{2+}$ signal by $\text{IP}_3$ uncaging on hyper-wrinkled cells.**

The movie sequence of images shows an osmotically wrinkled neutrophil that has been preloaded with caged  $\text{IP}_3$ . 405nm laser uncaging of  $\text{IP}_3$  (indicated by “uncaging pulse”) induces a cytosolic  $\text{Ca}^{2+}$  signal, evident by an increase in fluo4 intensity (green, left). Extended tubular blebs can be seen forming in the phase contrast sequence (right).

### **Movie 2: The effect of hyper-osmolarity on neutrophil kinesis**

The movie sequence of images shows the arrest of spontaneous kinesis by neutrophils subjected to a hyperosmotic step up from isotonic conditions (300mOsM, “ISO”) to hypertonic conditions (600mOsM, “HYPER”). Subsequent restoration of isotonicity (“ISO”) resulted in gradual restoration of cell movement, but cell polarity was lost.

### **Movie 3: Arrest of phagocytosis by hyperwrinkling**

The movie sequence shows the arrest of phagocytosis of a zymosan particle (ZYM) after the  $\text{Ca}^{2+}$  signal has been triggered by phagocytic cup formation, by an hyperosmotic step. The cytosolic  $\text{Ca}^{2+}$  is evident by the fluo4 intensity (green, left), and the progressive phagocytic cup formation is evident in the phase contrast sequence (PC, right) under isotonic conditions. Increasing the osmolarity by 300mOsM (“HYPER”) causes phagocytosis to cease to progress.

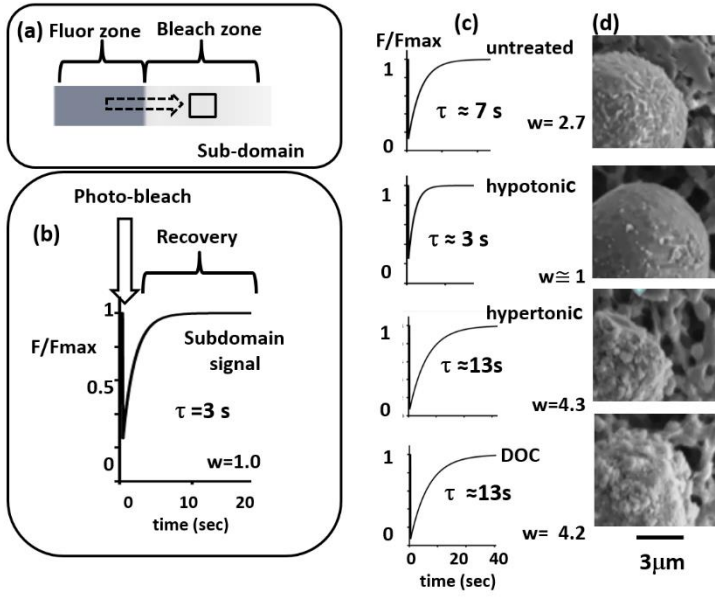


Figure 1

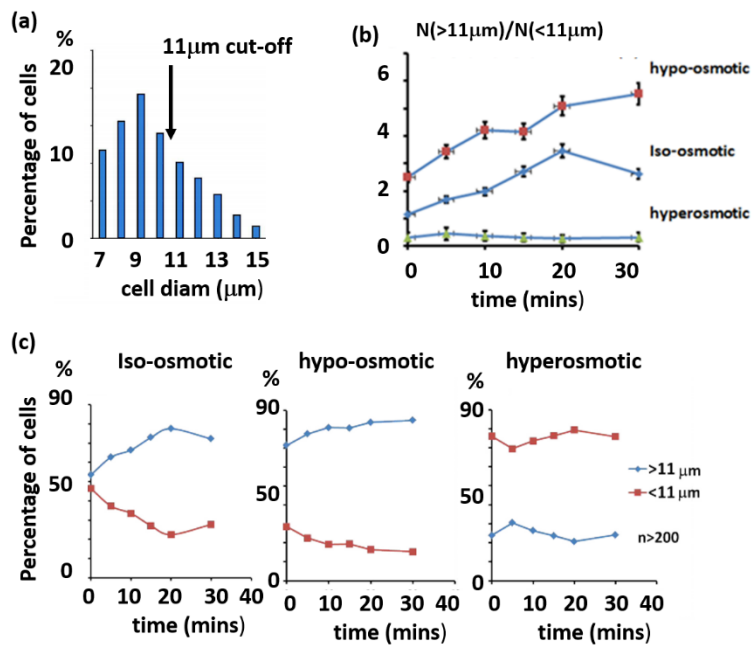


Figure 2

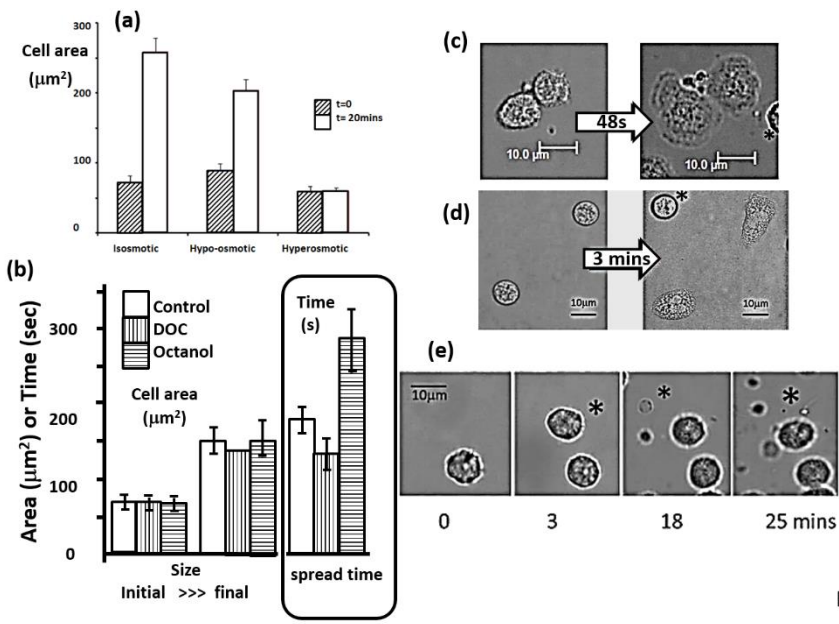


Figure 3

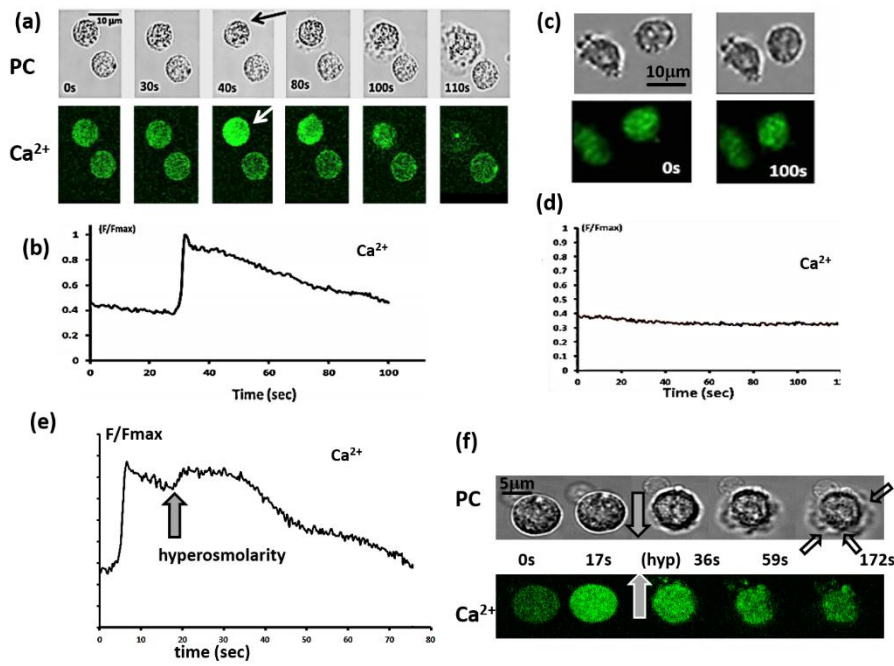


Figure 4

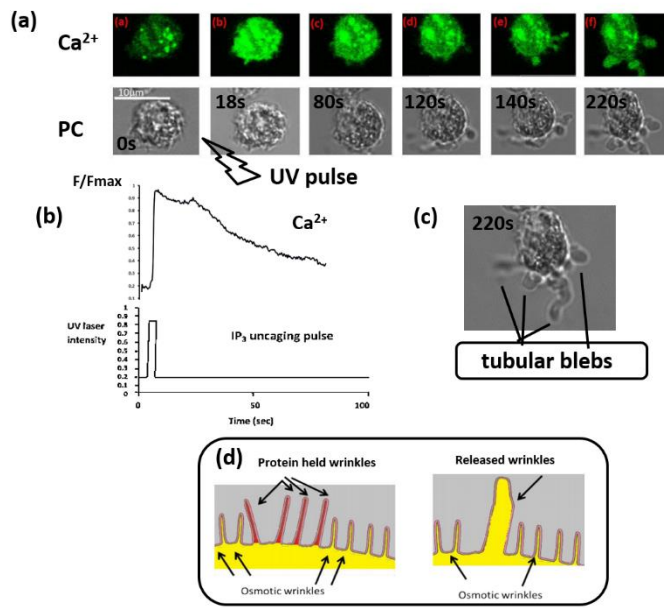


Figure 5

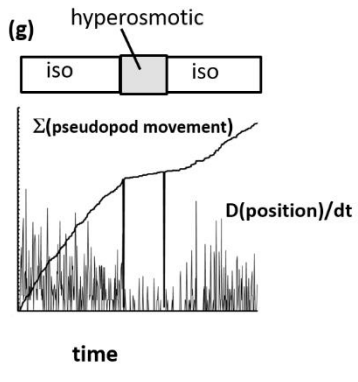
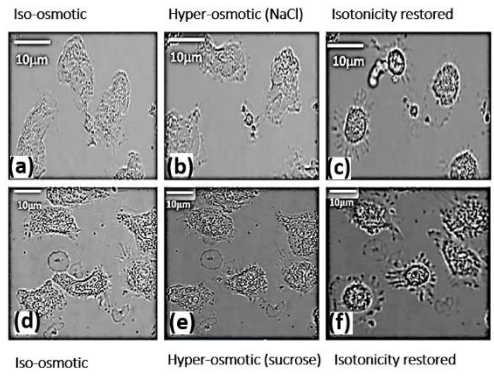
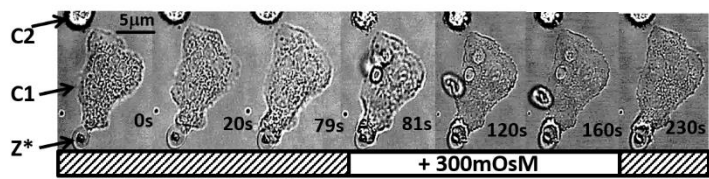


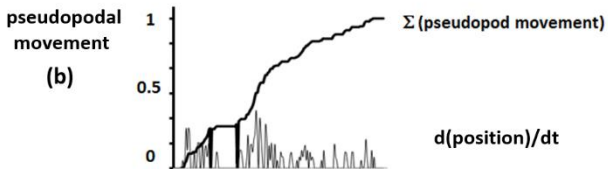
Figure 6



(a)

pseudopodal movement  $\Sigma$  (pseudopod movement)

(b)



(c)

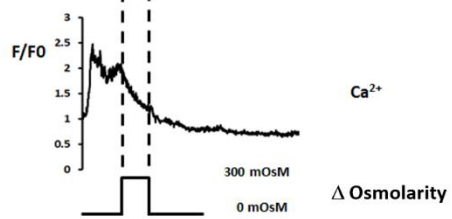


Figure 7

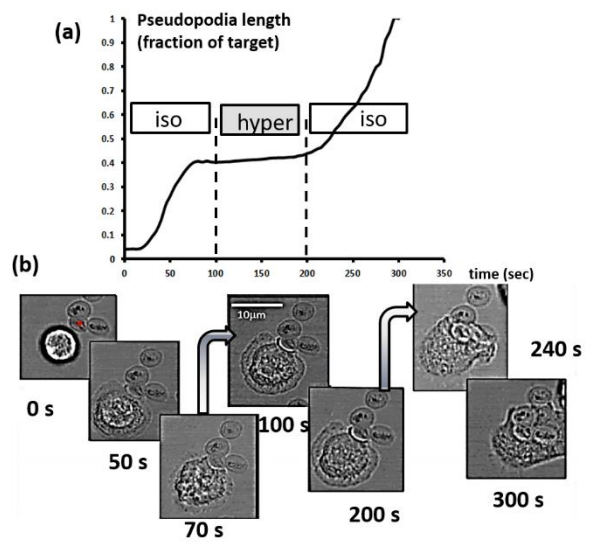
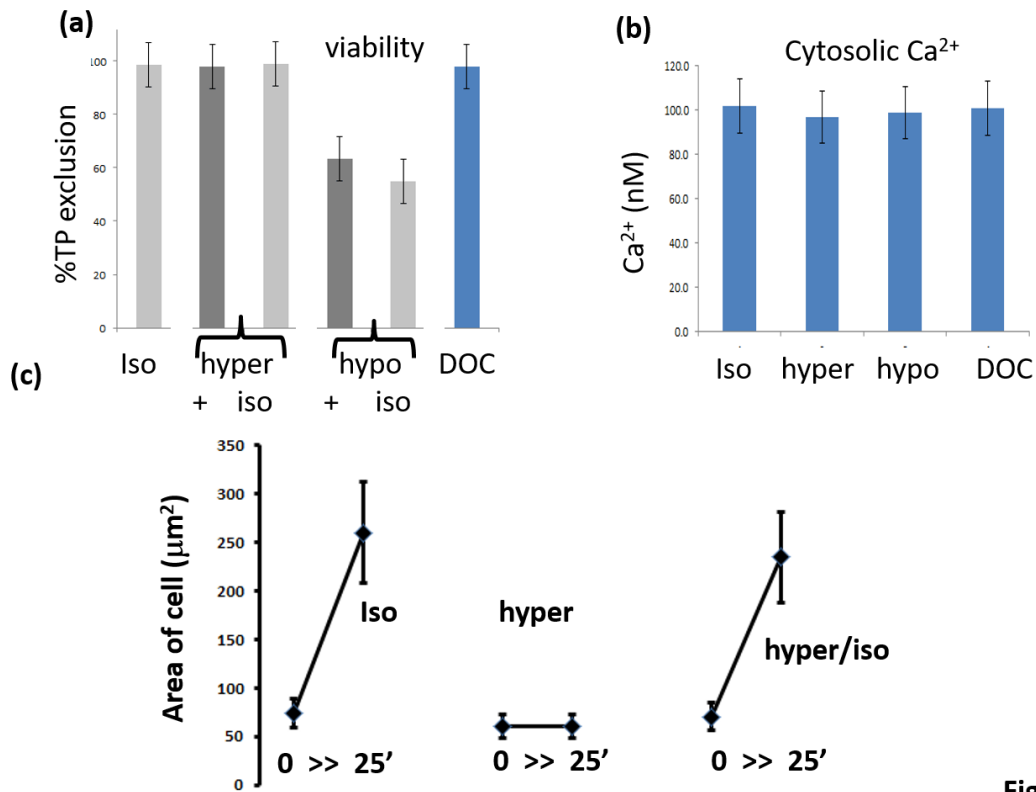


Figure 8

## Supplementary Material



**Fig S1**

**Fig S1 Experimental modification of neutrophil membrane topography: Viability of cells.** Cell viability as assessed by (a) trypan blue exclusion (%TP exclusion) in 2 separate experiments, (b) resting cytosolic Ca<sup>2+</sup> concentration, assessed by fluo4 intensity (n=20 cells) and (c) cell spreading, assessed by the area of the cell presents at time zero (at first contact with the substrate) and 25 mins later (25'). In all parts of the figure, the label “iso” indicates the data for cells in isotonic medium; “hyper” the data for cells in hypertonic medium; “hypo” the data for cells in hypotonic medium and “DOC” indicates cell pretreated with deoxycholate. (a) shows the data for the restoration of isotonicity after hypertonic or hypotonic medium of cells in suspension before retesting the spreading ability marked as “+” for the osmotic condition indicated and then “iso” for the same cells after restoration of isotonicity. (c) the spreading by the cells from the same populations of cells in isotonic (iso) hypertonic conditions (hyper: 25 mins) and then and after restoration of isotonicity (hyper/iso) before re-testing their spreading ability.

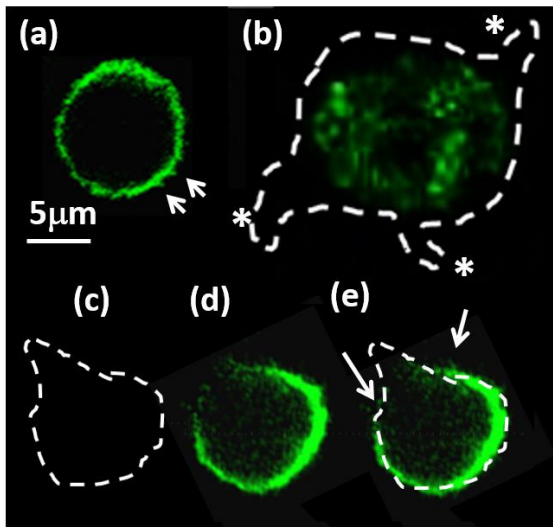


**Fig S2**

**Figure S2 Ezrin distribution in hyperwrinkled neutrophils during tubular bleb formation.** The distribution of ezrin was visualised by histochemistry of fixed cells (details in ref 18) where (a) shows the typical cortical distribution in spherical (hyperwrinkled, non spreading) cells with possible surface wrinkles indicated; (b) a shows a typical tubulated cell (outlined in the white dotted line, with the tubular blebs indicated by asterisks) with no cortical ezrin detected; (c) shows a cell with a single tubular bleb forming as shown in the cell outline (white dotted line); (d) the corresponding ezrin distribution; (e) shows the cell outline superimposed onto the ezrin distribution where the localised loss of ezrin is indicated by the arrows.

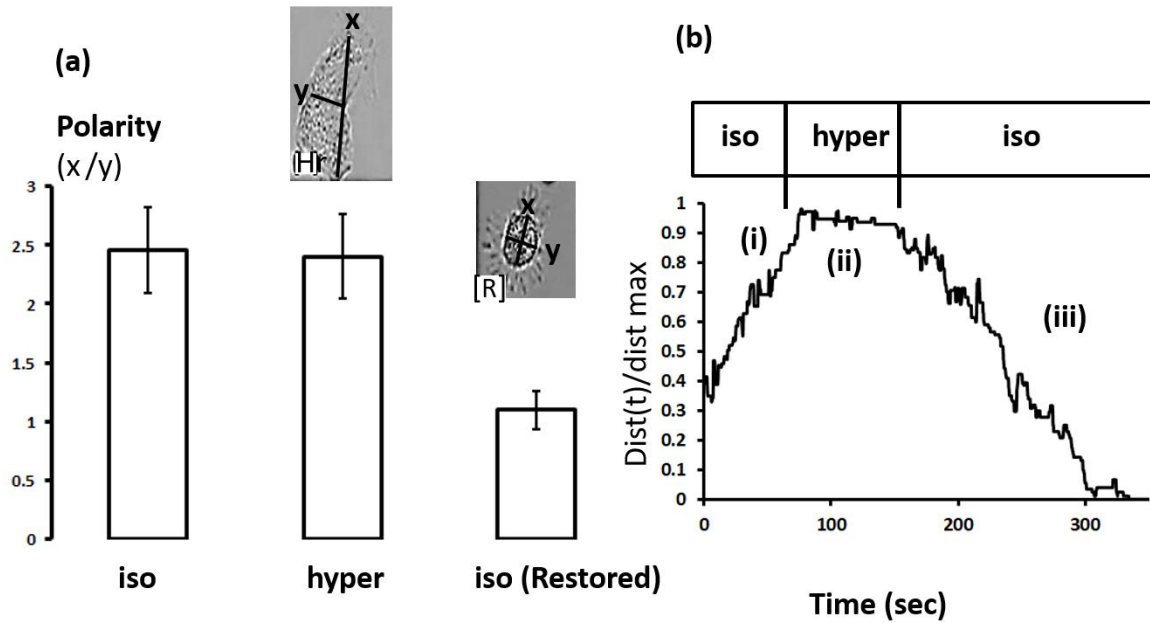


**Fig S3**

**Fig S3 Loss of polarity and directionality after restoration of isotonicity to hyperwrinkled neutrophils undergoing chemokinesis.** (a) Polarity was quantified as the ratio of the major axis (x) to the minor axis (y) as indicated in the image of a cell arrested in hypertonic medium (marked “H”) and the same cell after restoration of isotonicity (marked “R”). The data show the mean and SD of the polarity measurement from 14 cells in 3 separate experiments. (b) shows the movement of the cell edge of a neutrophil undergoing chemokinesis during the hypertonic and isotonicity restoration. The data shows the changing location of the cell edge as the distance from its final location at the times indicated, Dist (t) as a fraction of the maximum distance travel (dist<sub>max</sub>). The data, from a single representative cell, shows (i) the movement of the cell edge away from its final locus in isotonic medium, (ii) the arrest of movement during hypertonic hyper-wrinkling and (iii) the retraction of the cell edge towards its final location on restoration of isotonicity.

**Movie 1: Effect of induced  $\text{Ca}^{2+}$  signal by  $\text{IP}_3$  uncaging on hyper-wrinkled cells.**

The movie sequence of images shows an osmotically wrinkled neutrophil that has been preloaded with caged  $\text{IP}_3$ . 405nm laser uncaging of  $\text{IP}_3$  (indicated by “uncaging pulse”) induces a cytosolic  $\text{Ca}^{2+}$  signal, evident by an increase in fluo4 intensity (green, left). Extended tubular blebs can be seen forming in the phase contrast sequence (right).

**Movie 2: The effect of hyper-osmolarity on neutrophil kinesis**

The movie sequence of images shows the arrest of spontaneous kinesis by neutrophils subjected to a hyperosmotic step up from isotonic conditions (300mOsM, “ISO”) to hypertonic conditions (600mOsM, “HYPER”). Subsequent restoration of isotonicity (“ISO”) resulted in gradual restoration of cell movement, but cell polarity was lost.

**Movie 3: Arrest of phagocytosis by hyperwrinkling**

The movie sequence shows the arrest of phagocytosis of a zymosan particle (ZYM) after the  $\text{Ca}^{2+}$  signal has been triggered by phagocytic cup formation, by an hyperosmotic step. The cytosolic  $\text{Ca}^{2+}$  is evident by the fluo4 intensity (green, left), and the progressive phagocytic cup formation is evident in the phase contrast sequence (PC, right) under isotonic conditions. Increasing the osmolarity by 300mOsM (“HYPER”) causes phagocytosis to cease to progress.